Lawrence Berkeley National Laboratory

Title
Interplay between Swelling Kinetics and Nanostructure in Perfluorosulfonic Acid Thin-Films: Role of Hygrothermal Aging

Permalink
https://escholarship.org/uc/item/4r1005g0

Journal
ACS Applied Polymer Materials, 1(4)

ISSN
2637-6105

Authors
Tesfaye, Meron
Kushner, Douglas I
Kusoglu, Ahmet

Publication Date
2019-04-12

DOI
10.1021/acsapm.9b00005

Peer reviewed

On the Interplay between Swelling Kinetics and Nanostructure in PFSA Thin-films:

Role of Hygrothermal Ageing

Meron Tesfaye [†, ‡], Douglas I. Kushner [‡], Ahmet Kusoglu [‡, *]

[†] Chemical and Biomolecular Engineering, University of California Berkeley, Berkeley, CA, 94720

[‡] Energy Storage & Distributed Resources Division, Lawrence Berkeley National Laboratory, Berkeley, CA, 94720

[*]Author to whom correspondence should be addressed: akusoglu@lbl.gov

Abstract

Impacts of processing, storage, and operation on thin-film perflurosulfonic-acid (PFSA) ionomer coatings used in electrodes of electrochemical devices remains unestablished. In this work, alteration of structure-function relationship in ionomers is achieved via exposure to elevated temperature and humidity (hygrothermal ageing). Findings reflect a strong inverse correlation between ageing-induced ionomer thin-film domain orientation and water-transport kinetics evaluated from swelling. Impact of ageing is shown to be more pronounced on platinum, due to interactions with PFSA, as evidenced by greater increase in nano-domain orientation parallel to substrate accompanied by reduced water transport, in contrast to silicon support.
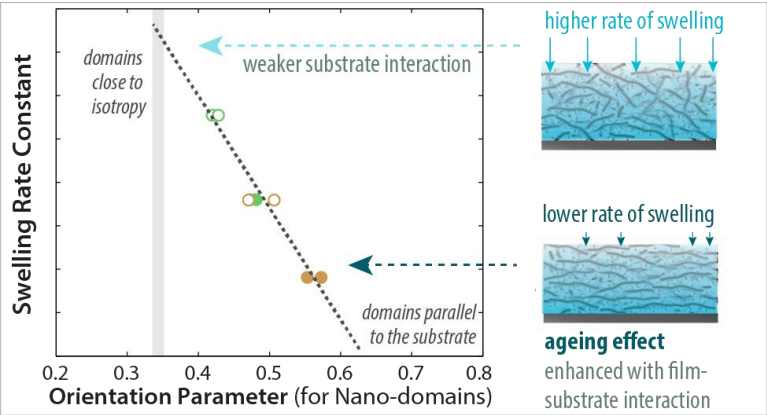
Table of Contents Graphic

28   Perfluorosulfonic-acid (PFSA) ionomers serve as benchmark polymer electrolytes

29   for various clean-water and energy-conversion electrochemical technologies.[1] Integral to

30   its ion- and water-transport capabilities is PFSA's phase-separated structure, which is

31   enhanced upon hydration of its -SO$_3$H end groups and maintained by the mechanical

32   stability of its inert backbone matrix.[1] As a random copolymer lacking well-defined

33   structure, comprehension of PFSA's intrinsic structure-function relationship has heavily

34   dependent on processing conditions (i.e. pre-treatment, cation contamination, *etc*.), thermal

35   history (unmanned, annealed, hot-pressed, *etc*.), and external stimuli (i.e. humidity, solvent,

36   *etc*.).[1,2] However, engineering high-performance ionomers requires establishment of

37   fundamental relationship between morphology of PFSA and properties that dictate

38   performance.[2] This is even more consequential for PFSA thin-films (nanometers in

39   thickness), as local interfaces and interactions impose additional constraints that limit

40   critical properties, impeding electrode performance in energy-conversion devices.[3,4]

41   Various examples of confinement-driven limitations in thin-film ionomers include

42   decreased water uptake, diffusivity, ion conductivity, accompanied by an overall increase

43   in transport resistance and mechanical stiffness.[1,3–7] While these property changes have

44   been ascribed to substrate-dependent morphological changes, interfacial interactions, and

45   finite-size driven enthalpic and entropic strains, few have resulted in definitive predictive

46   correlations.[5,8] To that effect, this study aims to explicitly correlate substrate-dependent

47   morphology (nano-structural orientation) with water-sorption kinetics (swelling property)

48   by employing hygrothermal ageing.

49   While some environmental conditions intrinsic to device operation (such as

50   hydration) are necessary to maintain PFSA functionality, they can also permanently alter

51 structure and functionality over time.[9–11] Notably, prolonged exposure of bulk PFSA to hot

52 and humid conditions (hygrothermal ageing) results in dramatic changes in ionomer

53 properties, altering ionomer's morphology, increasing mechanical properties and reducing

54 water uptake and conductivity.[9–13] Although no such explorations on the impact of ageing

55 in PFSA thin-films exists thus far, the technique of prolonged solvent exposure and

56 different processing conditions are frequently employed in block-copolymer thin-films to

57 access different morphologies.[14–16] In supported ionomer thin-films, similar to ionomers

58 present in electrodes, morphological changes cannot be decoupled from supporting

59 substrates. Recent findings have reported ionomer thin-film swelling property depends on

60 the chemical composition of substrates (platinum/oxidized platinum (Pt/PtO$_x$), gold (Au),

61 and carbon (C)), which may even be dictated during film formation, highlighting the key

62 role substrate interactions play in controlling film behavior.[3,7,17] Thin-films exhibit phase-

63 separated domains under humidification, similar to a membrane, but with anisotropy driven

64 by substrate and confinement effects.[3,18] While thin-films on silicon substrates with native

65 oxide (Si/SiO$_x$) exhibits close to isotropic patterns (random domain orientation), films on

66 hydrophobized Si or metallic substrates exhibit anisotropic domain orientation, which is

67 further enhanced for film thicknesses <50 nm.[1,3] This work demonstrates a direct link

68 between ionomer thin-film swelling, which serves as proxy for ion conductivity and water

69 transport, to substrate dependent nano-structural orientation as accessed by hygrothermal

70 ageing.

71   In this study, 30-40nm thin-films of PFSA with long- and medium-side-chain length

72 (Nafion and 3M respectively) were spun-cast on Si/SiO$_x$ and Pt/PtO$_x$ substrates to mimic

73 ionomers in electrochemical electrodes. The films were then hygrothermally aged for 2-4

74   days in an environmental chamber held at 85% relative humidity (RH) and a temperature

75   of 70 °C. Structural changes caused by hygrothermal ageing are investigated via *in-situ*

76   grazing incidence small-angle X-ray scattering (GISAXS). Fig. 1 summarizes the GISAXS

77   patterns of unaged (as-cast) and aged PFSA thin-films on Si/SiO_x and Pt/PtO_x support. An

78   ionomer peak (at q_{peak} = 2 to 2.5 nm^{-1}) is apparent in all, and more pronounced in aged thin-

79   films (Fig. 1a), signifying the phase-separated nanostructure with a correlation length of d

80   = $2\pi/q_{peak}$ = 2.5 to 3 nm. Upon hydration, the ionomer peak shifts to lower q (large d) due

81   to incorporation of water molecules into hydrophilic nano-domains. Interestingly, changes

82   in peak position as well as peak shape upon hydration are less distinct for aged films where

83   the hydrophilic-domain network appears to already be expanded and set as a result of

84   ageing.[3,18] (See SI for further discussion). The high-intensity regions around the specular

85   peak in the GISAXS images (Fig. 1a) highlight the hygrothermal ageing-induced

86   anisotropic structure. To analyze structural anisotropy, the intensity distributions around

87   the ionomer peak position (q_{peak} = 2.5 $\pm$ 0.25 nm^{-1}) are taken from the 2D GISAXS spectra

88   and plotted as a function of azimuthal angle, $I(\chi)$ (Fig. 1b). Films on the Si/SiO_x substrate

89   exhibit a low degree of anisotropy and closely follow the ideal isotropic distribution ($I(\chi)$

90   = constant). Hygrothermally-aged thin-films prepared on Pt/PtO_x exhibit an intensity

91   distribution, concentrated at q_P = 0, which indicates more domains are orientated parallel

92   to the surface. A domain orientation parameter, *O.P.*, quantifies the anisotropy of such

93   distributions:[3]

94
$$O.P. = \left\langle \cos^2 \chi \right\rangle = \frac{\int_0^{\pi/2} I(\chi)\sin(\chi)\cos^2\chi \, d\chi}{\int_0^{\pi/2} I(\chi)\sin(\chi) \, d\chi} \quad \langle S \rangle_{domain} = \frac{1}{2}\langle 3\omega_{ori} - 1 \rangle \qquad [1]$$

95   where *O.P.* is between 0 (domains perpendicular to the substrate) and 1 (domains parallel

96   to the substrate) and is 0.33 for an isotropic structure (random domain orientation). Fig. 1c

97   shows the *O.P.* for PFSA thin-films increases upon hygrothermal ageing. In addition, there

98   is a higher *O.P.* for aged long side-chain PFSA (Nafion over 3M), revealing the possible

99   role of pendant chain chemistry in these governing interactions.[18] Fig. 1c shows increased

100   nanostructural orientation on Pt/PtO$_x$ compared to Si/SiO$_x$, in both as-cast (unaged) and

101   aged state. Aged thin-films on Pt/PtO$_x$, also showed greater *O.P.* distribution probably due

102   to the dynamic interactions between water and Pt/ionomer interface.[3,17,19,20]

103

(a) 2D GISAXS Spectra

PFSA Film | Silicon   PFSA Film | Platinum

As-cast   As-cast

Aged   Aged

Aged - *Saturated*   Aged - *Saturated*

1D Intensity Profiles

Dry   *Saturated*

(b) Intensity Distribution (from GISAXS)

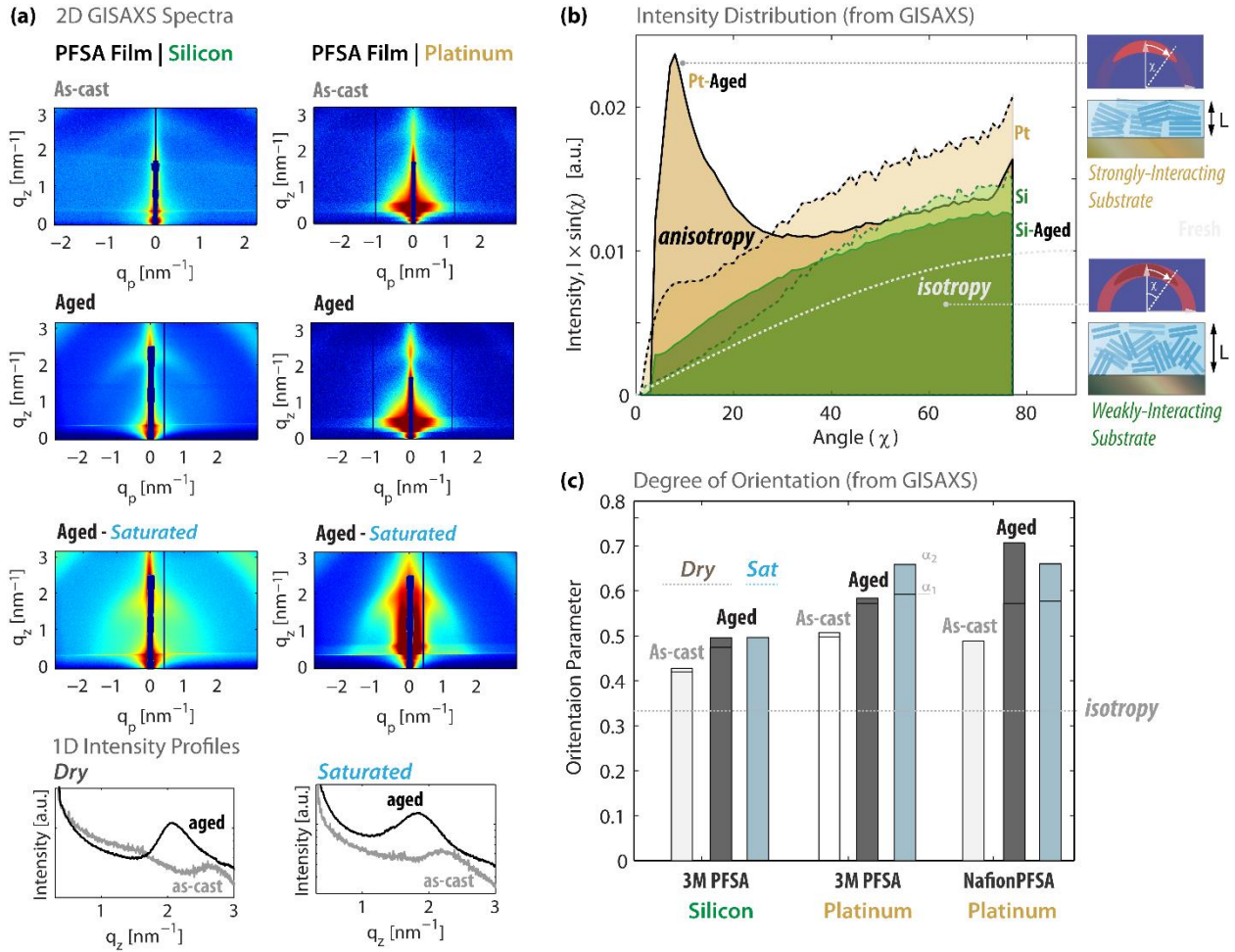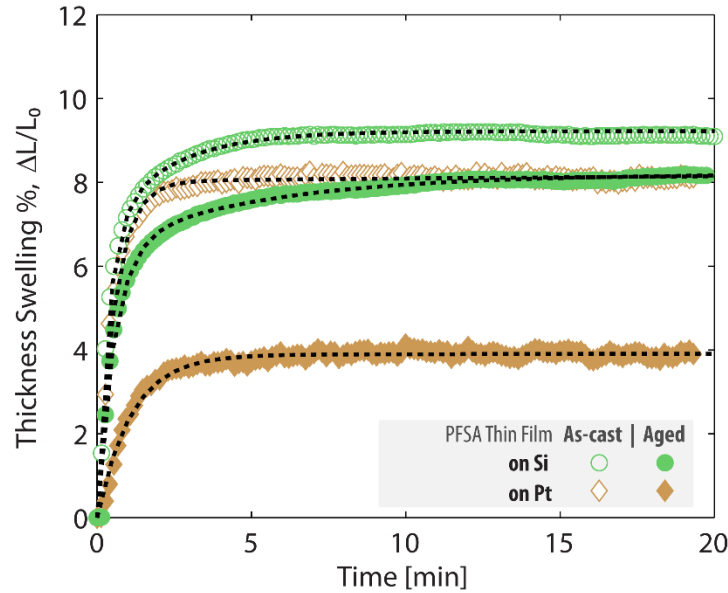**(c)** Degree of Orientation (from GISAXS)

104

Figure 1: (a) 2D GISAXS images of as-cast (unaged) and hygrothermally aged PFSA (3M, 825g/mol equivalent weight) thin-films spin-cast on Si/SiO_x and Pt/PtO_x substrate in dry (33%) and saturated (100% RH) conditions at 26 ℃. 1D intensity profiles are shown below for the 3M PFSA films on Si/SiO_x substrate, based on the 2D images. (b) Intensity distribution as a function of azimuthal angle, χ, for the ionomer peak. The solid and dashed lines represent the aged and as-cast samples, respectively, and the dotted line shows the distribution calculated for an ideal isotropic case. (c) Orientation parameter calculated from the distributions in (b). The low and high bars correspond to low and high incidence angle. (See SI for details).

The effect of hygrothermal ageing on ionomer swelling extent and kinetics was captured by *in-situ* spectroscopic ellipsometry. Fig. 2 compares swelling of aged and as-cast PFSA ionomer thin-films on Si/SiO_x and Pt/PtO_x substrates at 97% RH. In contrast to hygrothermally-aged films coated on Si/SiO_x, which show a 12% reduction in swelling, aged films on Pt/PtO_x exhibit a 50% reduction in extent of swelling normal to the substrate. For comparison, the same water-uptake reduction from reference (unaged) bulk PFSAs

119 (~50 µm thick) would require 100 days of hygrothermal ageing;[21] this difference between

120 bulk and thin-film aging highlights the enhanced interplay of confinement and substrate on

121 thin-film PFSAs. The effect of ageing is amplified on strongly-interacting substrates like

122 Pt/PtO$_x$,[3,17,19,22] which accelerates the ageing process.

123

124 Figure 2: Time-dependent fractional thickness swelling of PFSA (3M) thin-films (nominal
125 thickness, $L_0 \approx 34$ nm) spin cast on Si/SiO$_x$ and Pt/PtO$_x$ substrates during humidification from 0 to
126 97 % RH. Data are shown for as-cast (unaged) and aged (at 85% RH, 70 °C for 4 days) films. The
127 dashed lines are best-fit to the measured data (symbols) using a two-term exponential expression,
128 discussed later.

129 　　　　To quantify this explicitly, ageing-induced changes in thin-film nanostructure (Fig.

130 1) can be correlated with water-sorption dynamics by investigating swelling kinetics (Fig.

131 2). The time-dependent swelling process is analyzed by fitting the normalized transient

132 thickness change (Fig. 2) to a two-term exponential expression[1]:

$$\frac{L(t)-L_0}{L_\infty - L_0} = 1 - A\exp\left(-\frac{t}{\tau_1}\right) - (1-A)\exp\left(-\frac{t}{\tau_2}\right) \qquad [2]$$

133

134 where τ_1 and τ_2 are time constants for the short-term (fast, diffusional transport) and long-

135 term (slow, physical relaxation and interfacial transport) swelling processes,

136 respectively.[1,23] Fig. 3a shows the inverse time constant of water sorption kinetics, $k_s = 1/\tau$,

137 against $O.P.$ Assuming one-dimensional swelling in thin-films, interfacial transport and

138 water diffusion can be estimated from characteristic time constants τ_2 $(=L/k_{int})$ and τ_1

139 $(=L^2/D_{water})$, respectively. D_{water} in ionomer thin-films explored here ranges from 10^{-12} cm^2/s

140 to 10^{-13} cm^2/s; reduction in D_{water} tracks with increasing $O.P.$ and is on the same order of

141 magnitude as those reported by Eastman $et.$ $al.$[24] Unaged films on Pt/PtO$_x$ possess strong

142 orientation and ageing increases structural parallel orientation on both supports,

143 presumably impacting through-plane water transport. Considering the primary governing

144 water transport mechanism to be interfacial transport, $k_{int} = L/\tau_2$ (ranging from 10^{-6} to 10^{-8}

145 cm/s) illustrates a different aspect of ageing. Change in $O.P.$ is strongly coupled with

146 diffusional transport, which is accompanied by swelling at early times, while interfacial

147 relaxation becomes dominant at longer time-scales $(\tau_1 > \tau_2)$ and is dependent on $O.P.$ to a

148 lesser extent. For comparable ageing-induced change in $O.P.$, thin-films on Pt/PtO$_x$ show

149 higher time constant relative to Si/SiO$_x$, perhaps due to differences in substrate/ionomer

150 interaction compounded by physical ageing (relaxation) that has been shown to be

151 accelerated on metal supports.[20,22,25] However, the key takeaway is ageing-induced

152 morphological rearrangement ($O.P.$) is inversely correlated to characteristic rate for

153 swelling (k$_s$) representing water transport kinetics (or time constant is proportional to $O.P.$,

154 i.e., $\tau \propto 1/k_s \propto O.P.$).

(a) Swelling Kinetics vs. Nano-Domain Orientation

(b) Impact of annealing on thin film structure and swelling
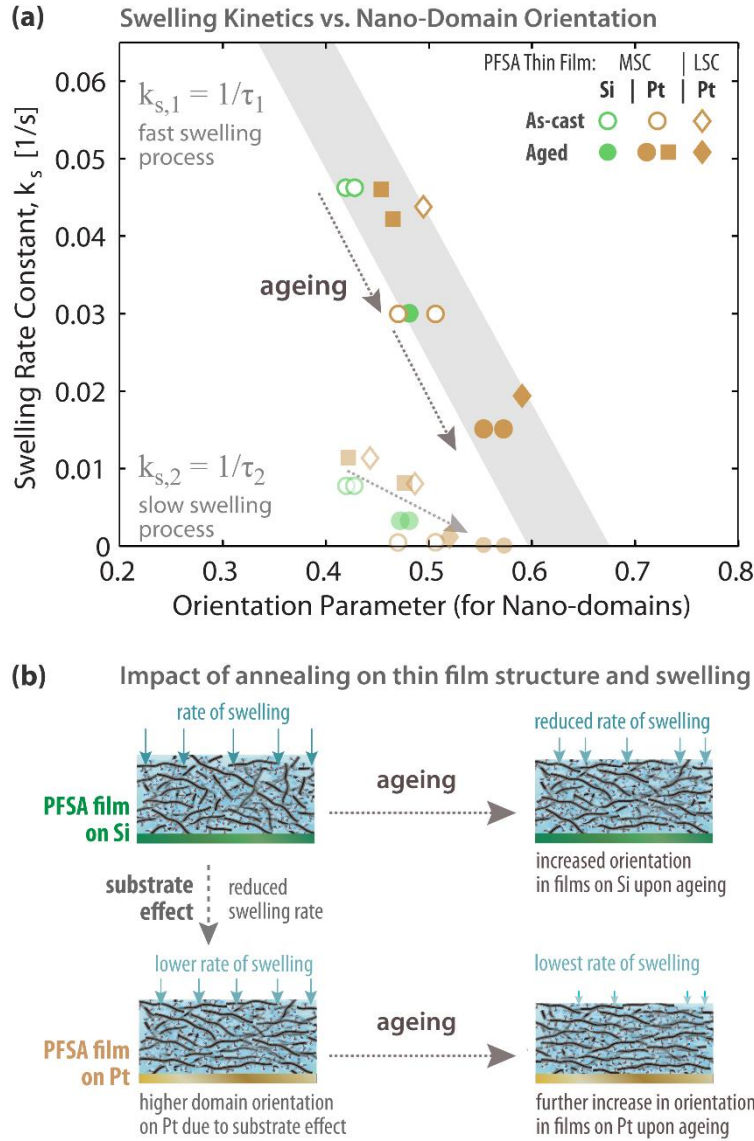

155

Figure 3: (a) Swelling rate constants of as-cast (unaged) and aged 3M (■,●) and Nafion (♦) PFSA thin-films during humidification to saturation (from ellipsometry) plotted against the orientation parameter of the same film in dry condition (from GISAXS). All the films were annealed after casting, except the unannealed 3M film on Pt (■), which is shown for comparison. Two rate constants are plotted for each case, representing the fast and slow swelling processes. (From Eq. (2)). (b) The schematics illustrate the inverse relationship between increasing domain orientation (parallel to the interfaces) and kinetics of swelling. The shaded region is shown as the guide for-the-eye.

164

165

166   Ionomer hydration controls transport properties like ion conduction and gas diffusion.

167 Tunable nanostructures that control hydration and transport pathways can be designed via

168 synthesis or processing techniques for well-ordered ionomers like sulfonated block or graft

169 copolymers.[2] A similar attempt is made here via hygrothermal ageing of disordered thin-

170 film PFSAs, whose properties are subject to additional surface interaction effects that are

171 heightened with finite size. Previous studies have demonstrated that alignment of

172 hydrophilic moieties at the ionomer surface, governed by the interactions of the ionomer

173 with vapor or liquid,[3,26–28] is related to mass-transport of water.[1,26,28] Findings in this work

174 reflect similar stimulus(hygrothermal ageing)-driven, surface(Pt/PtO$_x$)-controlled, and

175 chemistry (side-chain) influenced preferential orientation resulting in water transport

176 limitations in ionomer thin-films. A number of postulations are made here to explain this

177 direct correlation and reduction in ionomer water transport/swelling rate with increase in

178 *O.P.*:

179   (1) Increasing backbone alignment parallel to the substrate selectively lowers through-

180   plane water transport by lowering hydrophilic surface area and increasing tortuosity,

181   similar to the effect of structurally-induced orientation on ion transport.[7,8] Ageing-

182   induced chain orientation increases the fraction of -SO$_3^-$ moieties near the substrate,

183   intensifies their pairwise interactions, which could further enhance orientation, and

184   reduces swelling and swelling kinetics perpendicular to the substrate.

185   (2) Coupled with previous postulate on kinetics, hygrothermal ageing induces order in

186   the nanostructure, enabling the ionomer to access different quasi-equilibrium

187   states.[29] This is in similar vein to processing induced alignments in di-block

188   polymers.[2,16,30] Such a structure could preserve substrate/film interactions that

189   perpetuate and stabilize the chain configurations that could alter swelling governed

190   by thermodynamic equilibrium. Comparative ageing and morphological studies in

191   other solvents could elucidate the role of solvent and reversibility in achieving

192   alternative structures to decouple the kinetic and thermodynamic effects.

193   (3) Distinct from the other two possible explanations is sulfonic anhydride formation,

194   similar to that occurring in bulk PFSA.[9,10,21] Anhydride formation increases

195   equivalent weight via physical crosslinking of ionomer chains and reduces water

196   uptake. This explanation would imply that enhanced order and interaction on

197   Pt/PtO$_x$ accelerates anhydride formation in ionomer over Si/SiO$_x$ support.

198   Spectroscopic studies on aged thin-films could provide insight into presence of other

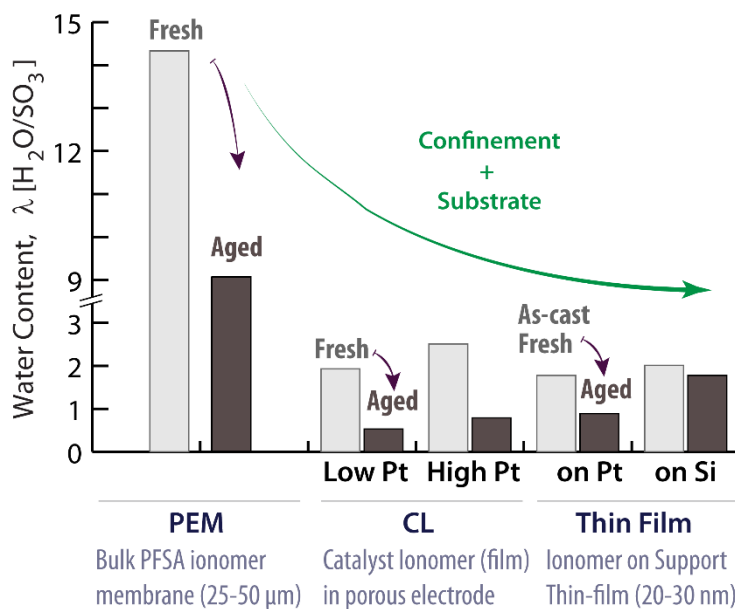199   forms of degradation and anhydride formation.

200

202   Figure 4: Comparison of maximum ionomer water content (at 95-97%RH) in bulk membrane,[10]
203   catalyst layer (CL), and thin-films on a support (PFSA for PEM is Nafion, while for CL and thin-
204   films 3M PFSA is used. See SI for full description of materials and treatment conditions).

205

206 These results on thin-film swelling are consistent with our hydration measurements on the

207 unaged and aged catalyst layers (CLs) of varying Pt loading (see SI); higher Pt loading

208 reflects significant reduction in water uptake with hygrothermal ageing compared to low-

209 loaded CL (Fig. 4). Thus, findings herein shed light into the ionomer structure-related

210 origins of the performance limitations in fuel-cell electrodes that may occur during

211 operation, and how they might be influenced by the dynamic substrate-ionomer

212 interactions. It must be noted that correlating ionomer's structure-swelling changes to

213 performance is not trivial due to variations in the Pt/ionomer interface such as surface

214 roughness (Figure S2 in Supporting Information) and substrate composition along with

215 environmental effects (reducing or oxidizing), which were shown to consequently alter

216 thin-film swelling.[17]

217   This letter reports compelling evidence for the existence of an explicit correlation

218 between the orientation of nano-domains and swelling kinetics in PFSA ionomer thin-films,

219 which is evidenced by ageing-induced changes in the film's nanostructure and swelling.

220 The higher the orientation parallel to film surface, the slower the transport normal to

221 surface. Stronger interactions between ionomer side-chains and Pt/PtO_x enhances the

222 impact of hygrothermal ageing by preferentially aligning more of the backbone parallel to

223 the substrate. Domain alignment and re-alignment caused by environment (e.g.,

224 hygrothermal ageing and saturation) and ionomer/substrate interactions dictates swelling

225 behavior and water transport in thin-films. Notably, the temperature used in this study for

226 ageing is much less than the initial annealing temperatures (70 ℃ vs. 140-160 ℃), which

227 underscores the role of water as an important stressor driving the film towards structural

228 reorganization that influence material properties. Results presented herein provide new

229 insights into the impact of environmental conditioning on inducing morphological changes

230 in ionomer thin-films, a phenomenon of great importance for elucidating and controlling

231 their structure/function relationship and transport response at dynamic interfaces in energy

232 conversion devices.

233

Acknowledgements

249 **Supporting Information**:

250 Associated Content: Full experimental methods are provided in detail in Supporting Information.

251

252 **Reference**

253 (1) Kusoglu, A.; Weber, A. Z. New Insights into Perfluorinated Sulfonic-Acid Ionomers.

254 *Chem. Rev.* **2017**, *117*, 987–1104.

255 (2) Park, M. J.; Hong, J.; Kim, S. Y. Role of Nanostructures in Polymer Electrolytes for

256 Energy Storage and Delivery. In *ACS Symposium Series 1096; Polymers for Energy*

257 *Storage and Delivery: Polyelectrolytes for Batteries and Fuel Cells*; 2012; pp 129–146.

258 (3) Kusoglu, A. Ionomer Thin Films in PEM Fuel Cells. In *Encyclopedia of Sustainability*

259 *Science and Technology*; Meyers, R., Ed.; Springer, New York, NY, 2018.

260 (4) Kongkanand, A.; Gu, W.; Mathias, M. F. Proton-Exchange Membrane Fuel Cells with

261 Low-Pt Content. In *Encyclopedia of Sustainability Science and Technology*; 2018.

262 (5) Tesfaye, M.; Kushner, D. I.; McCloskey, B. D.; Weber, A. Z.; Kusoglu, A. Thermal

263 Transitions in Perfluorosulfonated Ionomer Thin-Films. *ACS Macro Lett.* **2018**, 1237–

264 1242.

265 (6) DeCaluwe, S. C.; Baker, A. M.; Bhargava, P.; Fischer, J. E.; Dura, J. A. Structure-

266 Property Relationships at Nafion Thin-Film Interfaces: Thickness Effects on Hydration

267 and Anisotropic Ion Transport. *Nano Energy* **2018**, *46*, 91–100.

268 (7) Ono, Y.; Nagao, Y. Interfacial Structure and Proton Conductivity of Nafion at the Pt-

269 Deposited Surface. *Langmuir* **2016**, *32*, 352–358.

270 (8) Nagao, Y. Proton-Conductivity Enhancement in Polymer Thin Films. *Langmuir* **2017**, *33*,

271 12547–12558.

272 (9) Naudy, S.; Collette, F.; Thominette, F.; Gebel, G.; Espuche, E. Influence of Hygrothermal

Aging on the Gas and Water Transport Properties of Nafions Membranes. *J. Memb. Sci.* **2014**, *451*, 293–304.

(10)   Shi, S.; Dursch, T. J.; Blake, C.; Mukundan, R.; Borup, R. L.; Weber, A. Z.; Kusoglu, A. Impact of Hygrothermal Aging on Structure/Function Relationship of Perfluorosulfonic-Acid Membrane. *J. Polym. Sci. Part B Polym. Phys.* **2016**, *54*, 570–581.

(11)   Shi, S.; Chen, G.; Wang, Z.; Chen, X. Mechanical Properties of Nafion 212 Proton Exchange Membrane Subjected to Hygrothermal Aging. *J. Power Sources* **2013**, *238*, 318–323.

(12)   Onishi, L. M.; Prausnitz, J. M.; Newman, J. Water - Nafion Equilibria. Absence of Schroeder's Paradox. **2007**, 10166–10173.

(13)   Hensley, J. E.; Way, J. D.; Dec, S. F.; Abney, K. D. The Effects of Thermal Annealing on Commercial Nafion Membranes. *J. Memb. Sci.* **2007**, *298*, 190–201.

(14)   Stewart-Sloan, C. R.; Olsen, B. D. Protonation-Induced Microphase Separation in Thin Films of a Polyelectrolyte-Hydrophilic Diblock Copolymer. *ACS Macro Lett.* **2014**, *3*, 410–414.

(15)   Gu, X.; Gunkel, I.; Hexemer, A.; Russell, T. P. Controlling Domain Spacing and Grain Size in Cylindrical Block Copolymer Thin Films by Means of Thermal and Solvent Vapor Annealing. *Macromolecules* **2016**, *49*, 3373–3381.

(16)   Sinturel, C.; Vayer, M.; Morris, M.; Hillmyer, M. A. Solvent Vapor Annealing of Block Polymer Thin Films. *Macromolecules* **2013**, *46*, 5399–5415.

(17)   Tesfaye, M.; MacDonald, A. N.; Dudenas, P. J.; Kusoglu, A.; Weber, A. Z. Exploring

294   Substrate/Ionomer Interaction under Oxidizing and Reducing Environments. *Electrochem.*

295   *commun.* **2018**, *87*, 86–90.

296   (18) Kusoglu, A.; Dursch, T. J.; Weber, A. Z. Nanostructure/Swelling Relationships of Bulk

297   and Thin-Film PFSA Ionomers. *Adv. Funct. Mater.* **2016**, *26*, 4961–4975.

298   (19) Yagi, I.; Inokuma, K.; Kimijima, K.; Notsu, H. Molecular Structure of Buried

299   Perfluorosulfonated Ionomer/Pt Interface Probed by Vibrational Sum Frequency

300   Generation Spectroscopy. *J. Phys. Chem. C* **2014**, *118*, 26182–26190.

301   (20) Kodama, K.; Motobayashi, K.; Shinohara, A.; Hasegawa, N.; Kudo, K.; Jinnouchi, R.;

302   Osawa, M.; Morimoto, Y. Effect of the Side-Chain Structure of Perfluoro-Sulfonic Acid

303   Ionomers on the Oxygen Reduction Reaction on the Surface of Pt. *ACS Catal.* **2018**, *8*,

304   694–700.

305   (21) Collette, F. M.; Lorentz, C.; Gebel, G.; Thominette, F. Hygrothermal Aging of Nafion. *J.*

306   *Memb. Sci.* **2009**, *330*, 21–29.

307   (22) Selvan, M. E.; He, Q.; Calvo-Munoz, E. M.; Keffer, D. J. Molecular Dynamic Simulations

308   of the Effect on the Hydration of Nafion in the Presence of a Platinum Nanoparticle. *J.*

309   *Phys. Chem. C* **2012**, *116*, 12890–12899.

310   (23) Kongkanand, A. Interfacial Water Transport Measurements in Nafion Thin Films Using a

311   Quartz-Crystal Microbalance. *J. Phys. Chem. C* **2011**, *115*, 11318–11325.

312   (24) Eastman, S. A.; Kim, S.; Page, K. A.; Rowe, B. W.; Kang, S.; Soles, C. L.; Yager, K. G.

313   Effect of Confinement on Structure, Water Solubility, and Water Transport in Nafion Thin

314   Films. *Macromolecules* **2012**, *45*, 7920–7930.

315 (25) Kushner, D. I.; Hickner, M. A. Substrate-Dependent Physical Aging of Confined Nafion

316   Thin Films. *ACS Macro Lett.* **2018**, *7*, 223–227.

317 (26) Novitski, D.; Holdcroft, S. Determination of O2 Mass Transport at the Pt | PFSA Ionomer

318   Interface under Reduced Relative Humidity. *ACS Appl. Mater. Interfaces* **2015**, *7*, 27314–

319   27323.

320 (27) Hwang, G. S.; Parkinson, D. Y.; Kusoglu, A.; Macdowell, A. A.; Weber, A. Z.

321   Understanding Water Uptake and Transport in Nafion Using X-ray Microtomography.

322   *ACS Macro Lett.* **2013**, *2*, 288–291.

323 (28) He, Q.; Kusoglu, A.; Lucas, I. T.; Clark, K.; Weber, A. Z.; Kostecki, R. Correlating

324   Humidity-Dependent Ionically Conductive Surface Area with Transport Phenomena in

325   Proton-Exchange Membranes. *J. Phys. Chem. B* **2011**, *115*, 11650–11657.

326 (29) Kim, T. H.; Yi, J. Y.; Jung, C. Y.; Jeong, E.; Yi, S. C. Solvent Effect on the Nafion

327   Agglomerate Morphology in the Catalyst Layer of the Proton Exchange Membrane Fuel

328   Cells. *Int. J. Hydrogen Energy* **2017**, *42*, 478–485.

329 (30) Kim, J.; Kim, B.; Jung, B.; Kang, Y. S.; Ha, H. Y.; Oh, I. H.; Ihn, K. J. Effect of Casting

330   Solvent on Morphology and Physical Properties of Partially Sulfonated Polystyrene-

331   Block-Poly(Ethylene-Ran-Butylene)-Block-Polystyrene Copolymers. *Macromol. Rapid*

332   *Commun.* **2002**, *23*, 753–756.

333